AB INITIO THEORY OF PERPENDICULAR TRANSPORT IN METALLIC MAGNETIC MULTILAYERS

Josef Kudrnovský[1], Václav Drchal[1], Claudia Blaas[2], Peter Weinberger[2], Ilja Turek[3], and Patrick Bruno[4]

[1] *Institute of Physics, Academy of Sciences of the Czech Republic*
Na Slovance 2, CZ-182 21 Prague 8, Czech Republic
kudrnov@fzu.cz

[2] *Center for Computational Materials Science, Technical University of Vienna*
Getreidemarkt 9/158, A-1060 Vienna, Austria
cb@cms.tuwien.ac.at

[3] *Institute of Physics of Materials, Academy of Sciences of the Czech Republic*
Žižkova 22, CZ-616 62 Brno, Czech Republic
turek@ipm.cz

[4] *Max-Planck-Institut für Mikrostrukturphysik*
Weinberg 2, D-06120 Halle, Germany
bruno@mpi-halle.de

ABSTRACT

The current-perpendicular-to-plane (CPP) magnetoconductance of a sample sandwiched by two ideal non-magnetic leads is described at an *ab initio* level. The so-called 'active' part of the system is a trilayer consisting of two magnetic slabs of finite thickness separated by a non-magnetic spacer. We use a transmission matrix formulation of the conductance based on surface Green functions as formulated by means of the tight-binding linear muffin-tin orbital method. An equivalent and computationally more efficient formulation of the problem based on reflection matrices is also presented. The formalism is extended to the case of lateral supercells with random arrangements of atoms which in turn allows to deal with ballistic and diffusive transport on equal footing. Applications refer to fcc-based Co/Cu/Co(001) trilayers.

Properties of Complex Inorganic Solids 2, edited by A. Meike *et al.*
Kluwer Academic/Plenum Publishers, 2000

INTRODUCTION

Transport in layered materials is subject of intensive theoretical investigations, in particular in view of the discovery of the giant magnetoconductance (GMC) in metallic multilayers [1, 2]. Various theoretical treatments have been proposed, based on the semiclassical Boltzmann equation or, alternatively, on a Kubo-Greenwood type formulation within a free-electron model with random point scatterers, for the Kronig-Penney model, or within a single-band tight-binding model. A description of experimental and theoretical results can be found in a recent review article [3]. Up to now the GMC effect has been observed mostly in the diffusive transport regime in which the mean free path is much smaller than the dimension of the so-called 'active' part of the multilayer system, i.e., the whole system with exception of the leads. Most of measurements up to date were performed in the current-in-plane (CIP) geometry [1], the current-perpendicular-to-plane (CPP) geometry [2] seems to be experimentally more demanding. From a theoretical standpoint of view CPP transport is interesting because of an obvious role played by interfaces, its close relation to tunneling across an insulator or vacuum, and because of its relation to a semi-classical view of ballistic transport [4]. The present theoretical understanding of the CPP transport has been reviewed in a recent paper [5], including the transport in the ballistic regime. In this regime, in contrast to the diffusive regime, the mean free path is larger than the dimension of the 'active' part of the multilayer system. The spin-dependent scattering at ideal interfaces between magnetic and non-magnetic metals which form a multilayer, the so-called intrinsic potential scattering, is usually said to be the origin of the GMC in the ballistic regime [4]. In the diffusive regime the GMC is thought to originate from spin-dependent scattering off impurities in the bulk and/or at interfaces between the magnetic slabs and the spacer (extrinsic defects). It should be noted that in real multilayers also dislocations or stacking faults occur, and magnons and phonons can cause dynamical perturbations. While in the limiting cases of the strong diffusive regime and the ballistic regime simplifications can be made, a real multilayer system usually represents a mixture of both intrinsic and extrinsic defects.

Ab initio calculations of the GMC are still rather rare. We mention a Boltzmann-type approach developed for multilayer systems within the relaxation-time approximation, which is limited to either weak scattering or very low-concentration [6] limits. Typically, the electronic structure of a three-dimensional periodic (infinite) multilayer system is determined (velocities and the Fermi surface) and, in separate calculations, the spin-

dependent relaxation time of bulk impurities is found and used to solve the (classical) Boltzmann equation. Clearly, the change of the superlattice bandstructure due to impurities is neglected, hence the above mentioned limitation of the method. A solution of the Boltzmann equation for layered systems without the relaxation-time approximation has also been suggested [7]. Recently *ab initio* calculations using a Kubo-Greenwood approach generalized to layered systems [8, 9] have appeared in which (substitutional) disorder is included within an inhomogeneous coherent potential approximation (CPA). This is an appropriate approach to deal with the influence of imperfections and to treat intrinsic and extrinsic scattering on equal footing. However, up to now in there the so-called vertex corrections with respect to the configurational average of the products of two single particle Green functions are neglected. The above mentioned approaches can in principle be used for both the CIP and CPP geometry.

An alternative theoretical approach based on non-equilibrium Green functions or on a transmission matrix formalism (Landauer-type approach) can be used for the CPP transport. A useful review of these techniques can be found in a recent monograph [10].

It is the aim of this paper to formulate a surface Green function (SGF) approach to CPP transport in magnetic multilayers within the tight-binding linear muffin-tin orbital (TB-LMTO) method [11]. Related formulations based on empirical tight-binding (TB) models have appeared recently [13, 14, 15, 16]. The present formulation is then extended to the case of lateral two-dimensional supercells with random occupation of lattice sites by two kinds of atoms, whereby the stacking of such random layers in the growth direction can be arbitrary. The usefulness of such an approach has recently been illustrated for the case of a single-band TB model [17]. In particular it has been shown that current fluctuations due to different configurations are small for metallic multilayers if the size of the supercells is large enough. It should be mentioned, however, that in the case of tunneling through an amorphous spacer such fluctuations can be quite large [18]. We shall present an *ab initio* application of such an approach for the case of Co/Cu/Co(001)-based trilayers.

THEORY

Suppose the magnetic multilayer system consists of a semi-infinite left ($\mathcal{L}$) and a semi-infinite right ($\mathcal{R}$) non-magnetic lead sandwiching a trilayer consisting of a left and a right magnetic slab of varying thickness separated by a non-magnetic spacer again of varying thickness. The sequence of planes of atoms (layers) in the growth direction of the trilayer

is assumed to be arbitrary. In principle, atomic layers can be viewed in terms of $n \times n$ supercells ($n \times n$ two-dimensional complex lattice). In order to describe disorder (substitutional binary alloys) it is then necessary to average over different sizes n of supercells, and for each n over different occupations of the sites within the supercell by the two constituents involved. Quite clearly such an approach applies to disordered spacers and/or magnetic slabs as well as to disordered interfaces. In the following we neglect possible layer and lattice relaxations in the system; all formulations and calculations are based on a fcc Co(001) parent lattice.

ELECTRONIC STRUCTURE

The electronic structure of the system is described in terms of the following TB-LMTO Hamiltonian,

$$H^{\gamma,\sigma}_{\mathbf{R}L,\mathbf{R}'L'} = C^{\sigma}_{\mathbf{R}L}\,\delta_{\mathbf{R},\mathbf{R}'}\,\delta_{L,L'} + (\Delta^{\sigma}_{\mathbf{R}L})^{1/2}\left\{S^{\beta}\left(1-(\gamma^{\sigma}-\beta)\,S^{\beta}\right)^{-1}\right\}_{\mathbf{R}L,\mathbf{R}'L'}(\Delta^{\sigma}_{\mathbf{R}'L'})^{1/2}, \quad (1)$$

where $\mathbf{R}$ is the site index, σ is the spin index, and the potential parameters $C^{\sigma}_{\mathbf{R}L}$, $\Delta^{\sigma}_{\mathbf{R}L}$, and $\gamma^{\sigma}_{\mathbf{R}L}$ are diagonal matrices with respect to the angular momentum $L = (\ell m)$. The non-random screened structure constants matrix $S^{\beta}_{\mathbf{R}L,\mathbf{R}'L'}$ and the site-diagonal screening matrix $\beta_{\mathbf{R},LL'} = \beta_L\,\delta_{L,L'}$ are spin-independent. Assuming one and the same two-dimensional translational symmetry in each atomic layer p, $\mathbf{k}_{||}$-projections can be defined, where $\mathbf{k}_{||}$ is a vector from the corresponding surface Brillouin zone (SBZ). In a principal layer formalism [11], the screened structure constants $S^{\beta}_{p,q}$ are of block tridiagonal form. Neglecting layer relaxations they are given by

$$S^{\beta}_{p,p}(\mathbf{k}_{||}) = S^{\beta}_{0,0}(\mathbf{k}_{||}),\quad S^{\beta}_{p,q}(\mathbf{k}_{||}) = S^{\beta}_{0,1}(\mathbf{k}_{||})\,\delta_{p+1,q} + S^{\beta}_{1,0}(\mathbf{k}_{||})\,\delta_{p-1,q}\,. \quad (2)$$

The properties of individual atoms occupying lattice sites are characterized by potential function matrices,

$$P^{\beta,\sigma}_{\mathbf{R}}(z) = \frac{z - C^{\sigma}_{\mathbf{R}}}{\Delta^{\sigma}_{\mathbf{R}} + (\gamma^{\sigma}_{\mathbf{R}} - \beta)\,(z - C^{\sigma}_{\mathbf{R}})}\,, \quad (3)$$

which are diagonal with respect to L and are obtained by solving the corresponding Kohn-Sham equations. The potential functions assume the same value $P^{\beta,\sigma}_{p}(z)$ for each site within a given atomic layer p for

1×1-supercells, and, in principle, n^2 different values $P_{p,i}^{\beta,\sigma}(z)$ for $n \times n$-supercells. Finally, we define the infinite (screened) Green function matrix $g^{\beta,\sigma}(z)$ in the TB-LMTO method as

$$\left(g^{\beta,\sigma}(\mathbf{k}_{||}, z)\right)_{p,q}^{-1} = P_p^{\beta,\sigma}(z)\,\delta_{p,q} - S_{p,q}^{\beta}(\mathbf{k}_{||})\,. \tag{4}$$

Assuming that the 'active' part of the multilayer system consists of N layers and that the physical properties of all lead layers are identical, we can characterize these layers by so-called embedding potentials $\Gamma_p^{\beta,\sigma}$ [11], which for $p = 1$ and $p = N$ are given by

$$\begin{aligned} \Gamma_1^{\beta,\sigma}(\mathbf{k}_{||}, z) &= S_{1,0}^{\beta}(\mathbf{k}_{||})\,\mathcal{G}_{\mathcal{L}}^{\beta,\sigma}(\mathbf{k}_{||}, z)\,S_{0,1}^{\beta}(\mathbf{k}_{||})\,, \\ \Gamma_N^{\beta,\sigma}(\mathbf{k}_{||}, z) &= S_{0,1}^{\beta}(\mathbf{k}_{||})\,\mathcal{G}_{\mathcal{R}}^{\beta,\sigma}(\mathbf{k}_{||}, z)\,S_{1,0}^{\beta}(\mathbf{k}_{||})\,, \end{aligned} \tag{5}$$

and which are zero otherwise. The quantities $\mathcal{G}_{\mathcal{X}}^{\beta,\sigma}$, $\mathcal{X} = \mathcal{L}, \mathcal{R}$, are the corresponding SGFs of the ideal left and right leads.

The layer-diagonal blocks of the inverse of the Green function matrix can then be written as

$$\begin{aligned} \left(g^{\beta,\sigma}(\mathbf{k}_{||}, z)\right)_{p,p}^{-1} &= P_1^{\beta}(z) - S_{0,0}^{\beta,\sigma}(\mathbf{k}_{||}) - \Gamma_1^{\beta,\sigma}(\mathbf{k}_{||}, z) \quad \text{for } p = 1\,, \\ \left(g^{\beta,\sigma}(\mathbf{k}_{||}, z)\right)_{p,p}^{-1} &= P_p^{\beta}(z) - S_{0,0}^{\beta,\sigma}(\mathbf{k}_{||}) \quad \text{for } 1 < p < N\,, \\ \left(g^{(0,\sigma)}(\mathbf{k}_{||}, z)\right)_{p,p}^{-1} &= P_N^{\beta}(z) - S_{0,0}^{\beta,\sigma}(\mathbf{k}_{||}) - \Gamma_N^{\beta,\sigma}(\mathbf{k}_{||}, z) \quad \text{for } p = N\,, \end{aligned} \tag{6}$$

while its off-diagonal blocks are given by

$$\left(g^{\beta,\sigma}(\mathbf{k}_{||}, z)\right)_{p,q}^{-1} = -S_{0,1}^{\beta}(\mathbf{k}_{||})\,\delta_{p+1,q} - S_{1,0}^{\beta}(\mathbf{k}_{||})\,\delta_{p-1,q}\,. \tag{7}$$

It should be noted that Eqs. (4–7) only apply in the case of an infinite parent lattice (no layer relaxations). In this way the originally infinite matrix can easily be reduced to a finite matrix with the embedding potentials acting as boundary conditions. The block-tridiagonal form in Eq. (7) of the inverse of the Green function allows to use efficient methods [11, 12] to determine any non-vanishing block of $g_{p,q}^{\beta,\sigma}(\mathbf{k}_{||}, z)$. In particular, this applies to the blocks $g_{1,N}^{\beta,\sigma}(z)$, $g_{N,1}^{\beta,\sigma}(z)$, and/or $g_{N,N}^{\beta,\sigma}(z)$ which are needed for the evaluation of the GMC described in the next subsection. We refer the reader to a recent book [11] for further details concerning the TB-LMTO method for layered systems.

In the case of two-dimensional $n \times n$ (lateral) supercells the above expressions remain formally the same, however, each quantity is now

replaced by a supermatrix labelled by the positions of the sites within a given supercell. In the case of binary substitutional alloys the corresponding potential functions are assumed to have only two different values for the two constituents involved, i.e., we neglect possible local environment effects and short-range order within a given supercell. It should be noted that, in principle, for each chosen supercell all inequivalent potential functions have to be determined selfconsistently.

MAGNETOCONDUCTANCE

Our derivation of the conductance C_M follows that given in [13]. Its details will be published elsewhere. In the following a subscript M=F (AF) denotes the ferromagnetic (antiferromagnetic) configuration of the magnetizations in the magnetic slabs, respectively.

The resulting expression for the conductance per interface atom is given by

$$C_M = \sum_\sigma C_M^\sigma \,, \quad C_M^\sigma = \frac{e^2}{h} \frac{1}{N_{||}} \sum_{\mathbf{k}_{||}} T_M^\sigma(\mathbf{k}_{||}, E_F) \,, \tag{8}$$

where $N_{||}$ is the number of $\mathbf{k}_{||}$-points in the SBZ and E_F is the Fermi energy. Suppressing the subscript M the transmission coefficient $T^\sigma(\mathbf{k}_{||}, E)$ can be expressed as

$$T^\sigma(\mathbf{k}_{||}, E) = \lim_{|\delta|\to 0} \mathrm{tr} \{ B_1^{\beta,\sigma}(\mathbf{k}_{||}, E)\, g_{1,N}^{\beta,\sigma}(\mathbf{k}_{||}, z_+) \times B_N^{\beta,\sigma}(\mathbf{k}_{||}, E)\, g_{N,1}^{\beta,\sigma}(\mathbf{k}_{||}, z_-) \} \,, \tag{9}$$

where tr denotes the trace over angular momenta,

$$\begin{aligned} B_1^\sigma(\mathbf{k}_{||}, E) &= i \left(\Gamma_1^{\beta,\sigma}(\mathbf{k}_{||}, z_+) - \Gamma_1^{\beta,\sigma}(\mathbf{k}_{||}, z_-) \right) \,, \\ B_N^\sigma(\mathbf{k}_{||}, E) &= i \left(\Gamma_N^{\beta,\sigma}(\mathbf{k}_{||}, z_+) - \Gamma_N^{\beta,\sigma}(\mathbf{k}_{||}, z_-) \right) \,, \end{aligned} \tag{10}$$

and $z_\pm = E \pm i\delta$. In this formulation we have assumed a collinear spin structure and that the spin σ is a good quantum number. This assumption is valid only for collinear spin structures if the spin-orbit interaction is neglected. The magnetoconductance ratio is then defined as

$$GMC = (C_\mathrm{F}^\uparrow + C_\mathrm{F}^\downarrow)/(C_\mathrm{AF}^\uparrow + C_\mathrm{AF}^\downarrow) - 1 \,. \tag{11}$$

The reflection and transmission coefficients are related by

$$R^\sigma(\mathbf{k}_{||}, E) = 1 - T^\sigma(\mathbf{k}_{||}, E) \,, \tag{12}$$

and can be expressed as (I is the unit matrix)

$$R^{\sigma}(\mathbf{k}_{||},E) = \lim_{|\delta|\to 0} \mathrm{tr}\,\{\Big[B_N^{\sigma}(\mathbf{k}_{||},E)\, g_{N,N}^{\beta,\sigma}(\mathbf{k}_{||},z_+) + i\,I\Big] \times \Big[B_N^{\sigma}(\mathbf{k}_{||},E)\, g_{N,N}^{\beta,\sigma}(\mathbf{k}_{||},z_-) - i\,I\Big]\}\,, \qquad (13)$$

such that the magnetoconductance can be evaluated using the layer-diagonal blocks of the Green function matrix $g^{\beta,\sigma}(z)$ rather than the layer off-diagonal blocks as in the case of the transmission coefficient [13].

There exists, however, a direct way of expressing the transmission coefficient $T^{\sigma}(\mathbf{k}_{||},E)$ in terms of the layer-diagonal blocks of the system Green function $g^{\beta,\sigma}(z)$, namely,

$$T^{\sigma}(\mathbf{k}_{||},E) = \lim_{|\delta|\to 0} \mathrm{tr}\,\{\tilde{B}_N^{\sigma}(\mathbf{k}_{||},E)\, g_{N,N}^{\beta,\sigma}(\mathbf{k}_{||},z_+) \times B_N^{\sigma}(\mathbf{k}_{||},E)\, g_{N,N}^{\beta,\sigma}(\mathbf{k}_{||},z_-)\}\,, \qquad (14)$$

where B_N^{σ} is defined in Eq. (10), and $\tilde{B}_N^{\sigma}$ is given by

$$\tilde{B}_N^{\sigma}(\mathbf{k}_{||},E) = i\,\left(\tilde{\Gamma}_N^{\beta,\sigma}(\mathbf{k}_{||},z_+) - \tilde{\Gamma}_N^{\beta,\sigma}(\mathbf{k}_{||},z_-)\right)\,, \qquad (15)$$

where $\tilde{\Gamma}_N^{\beta,\sigma}$ is the embedding potential of the semi-infinite 'fragment' to the left of the last layer in the trilayer system.

The generalization of the formalism to the supercell case proceeds similarly to the previous section: the corresponding matrices are substituted by supermatrices labelled by individual atoms within a supercell and the $\mathbf{k}_{||}$-integration is confined to the (n^2-times smaller) SBZ corresponding to the supercell. However, the computational effort within the present SGF technique can significantly be reduced by using the fact that the SGFs are independent of the choice of a supercell, since the atomic position vectors within a given supercell are nothing but lattice vectors of the two-dimensional lattice that corresponds to the parent lattice (1×1-supercell) of the leads. One can express the supercell (sc) SGF therefore in terms of the SGF of the original lattice as follows

$$\mathcal{G}_{K,K'}^{sc}(\mathbf{q}_{||},z) = \sum_{\mathcal{R}_K} \mathrm{e}^{-i\,\mathbf{q}_{||}\,(\mathcal{R}_K-\mathcal{R}_{K'})}\,\mathcal{G}_{\mathcal{R}_K,\mathcal{R}_{K'}}^{sc}(z)\,,$$

$$\mathcal{G}_{\mathcal{R}_K,\mathcal{R}_{K'}}^{sc}(z) = \frac{1}{N_{||}} \sum_{\mathbf{k}_{||}}^{\mathrm{SBZ}} \mathrm{e}^{i\,\mathbf{k}_{||}\,(\mathcal{R}_K-\mathcal{R}_{K'})}\,\mathcal{G}(\mathbf{k}_{||},z)\,, \qquad (16)$$

where $\mathbf{k}_{||}$ and $\mathbf{q}_{||}$ denote vectors in the SBZ of the original lattice and in the supercell SBZ, respectively, and the $\mathcal{R}_K$ refer to atomic positions within the supercell.

The computational scheme described above can be used also for supercell studies based on a single-band TB model. Assuming a nearest-neighbor hopping parameter t and identical left and right leads, we obtain [17]

$$T^{\sigma}(\mathbf{k}_{||}, E) = t^2 \, |A^{\sigma}(\mathbf{k}_{||}, E) \, g^{\sigma}_{1,N}(\mathbf{k}_{||}, z_+)|^2 \,, \tag{17}$$

where

$$A^{\sigma}(\mathbf{k}_{||}, E) = -\frac{1}{\pi} \operatorname{Im} \mathcal{G}^{\sigma}(\mathbf{k}_{||}, E + i\delta) \tag{18}$$

are the Bloch spectral functions of the corresponding SGF $\mathcal{G}^{\sigma}(\mathbf{k}_{||}, z)$ for the leads.

RESULTS AND DISCUSSION

We have performed calculations for the following formal multilayer system:

Cu(001) semi-infinite lead	$\Vert$	M_m magnetic slab	S_s spacer	M_m magnetic slab	$\Vert$	Cu(001) semi-infinite lead

(19)

where $N = 2m+s$. For $Co_m/Cu_s/Co_m$ trilayers we have studied: (i) the dependence of the GMC on the thickness of magnetic slabs m and (ii) the oscillatory behavior of the GMC as a function of the spacer thickness s. Furthermore, we have studied (iii) the oscillatory behavior of the GMC as a function of the spacer thickness for a (CuPd) superstructure spacer, namely, $Co_m/(CuPd)_r/Co_m$ trilayers, where r is the number of repetitions. If s is an even number then the superstructure is terminated by a Pd layer, if s is odd the terminating layer is formed by Cu atoms. The combined effect of intrinsic and extrinsic defects will be demonstrated for Co/Cu/Co-based trilayers on the following cases: (i) interdiffused interfaces; (ii) a random spacer sandwiched by ideal magnetic slabs; (iii) an ideal Cu spacer sandwiched by disordered magnetic slabs; and (iv) a case with combined disorders of types (ii) and (iii).

NUMERICAL IMPLEMENTATION

Random substitutional alloys $A_{1-x}B_x$ are simulated by random supercells with the same average composition. Random configurations were generated using the RM48 random number generator [19] and the binary correlation function was evaluated to test the 'randomness' of each configuration. For the single-band TB model we have tested $n \times n$ random supercells (n=5, 7, 10) corresponding roughly to a $A_{85}B_{15}$ random substitutional alloy, namely, 21 A atoms and 4 B atoms for the 5×5-supercell and 41 A atoms and 8 B atoms for the 7×7-supercell randomly

distributed over the sites within the supercell. In the case of the TB-LMTO model we have tested only 5×5- and 7×7-supercells. In all cases (typically an average over 5 configurations for a 5×5-supercell and an average over 3 configurations for a 7×7-supercell were calculated) the results for the partial currents agreed within 1–3%, the agreement being better for larger supercells. The same random supercells were used for both the single-band model and the TB-LMTO studies.

In principle, one should use selfconsistent potential parameters corresponding to a given random supercell, however, such an approach is numerically prohibitive for 5×5- or 7×7-supercells. For the case of a 2×2-supercell and $A_{75}B_{25}$ alloys we found that the fluctuations of the calculated potential parameters for A and B atoms for different random configurations from those obtained selfconsistently using the CPA are quite small (of the order of a few per cent). We have thus used the selfconsistent CPA potential parameters determined for a given alloy composition [11] also in the present supercell calculations. It should be noted that the same parameters were employed for various random configurations as well as for different supercell sizes. We have thus neglected all possible fluctuations of the potential parameters due to a variation of the local environment and assumed that the potential parameters take only two values the same for any A and B atom within a supercell. The potential parameters used are those of the corresponding A/B interface (ideal or random) where A(B) corresponds to atoms forming magnetic (spacer) layers. We have also neglected the layer dependence of the potential parameters and chosen their bulk-like values.

The $\mathbf{k}_{||}$-integration covers 10000 points in the full fcc(001)-SBZ (400 (196) points in the corresponding 5×5- (7×7)-supercell SBZ). In some cases, in particular in the ballistic regime a much higher number of $\mathbf{k}_{||}$-points was used to obtain well converged results. In all cases we have employed $|\mathrm{Im}z_{\pm}| = 10^{-7}$ Ry. It should be noted that for a 1×1-supercell one can integrate over the irreducible part of the SBZ while for the random supercell the $\mathbf{k}_{||}$-integration is confined to the full supercell SBZ (or, more precisely, over a half of the supercell SBZ due to time-reversal symmetry).

BALLISTIC TRANSPORT

We shall start our discussion by a remark concerning some general features of the electronic structure of Cu bands and of Co spin-up (↑) and Co spin-down (↓) bands at the Fermi energy of Cu leads. It should be noted that by 'bands' we mean the bands of the three-dimensional periodic bulk systems fcc Cu and fcc Co (at the Fermi energy of Cu).

The Cu- and Co↑-bands are very similar representing only a very weak intrinsic scattering potential at the Cu/Co interface. Consequently, the transmission of ↑-electrons for a ferromagnetic alignment of the magnetizations (and hence also their conductance as given by Eq. (8)) through the Co/Cu interfaces is large. On the contrary, the large difference between the Cu- and Co↓-bands acts as an effective potential barrier at the interface for ↓-electrons and, hence, gives rise to much smaller F↓- and AF-conductances. It should be also noted that in this paper we will study only symmetrical trilayers, i.e., the case of identical left and right magnetic slabs for which spin-up and spin-down conductances for the AF alignments coincide.

The dependence of the GMC of ideal $Co_m/Cu_5/Co_m$ trilayers on the thickness of the magnetic slabs m is presented in Fig. 1. The most remarkable feature is a strong suppression of the GMC (Fig. 1a) for small thicknesses of the magnetic slabs and a saturation of about 100% at large thicknesses. This result can be understood by plotting partial conductances, namely the F↑- and F↓-conductances for the ferromagnetic alignment of the magnetizations in the left and the right magnetic slabs and that for the antiferromagnetic alignment (AF-conductances). The suppression of the GMC is quite likely due to an effective potential barrier in the d↓-channel because of the above mentioned large difference between the Cu- and Co↓-bands. Hence, a narrower magnetic slab allows for a larger transmission of electrons, in particular for the F↓-conductance and both AF-conductances. As a result, the total AF-conductance increases faster than the total F-conductance and hence the GMC ratio drops (see also [16]). The oscillatory behavior of the conductances can be related to the oscillatory behavior of the F↓-conductances of a single Co slab of varying thickness embedded into the Cu host (Fig. 1b, empty symbols). Quite clearly such oscillations can be ascribed to multiple scattering effects of ↓-electrons at the interfaces. The GMC of finite Co slabs never reaches the limit of semi-infinite Co slabs because of different ballistic conductances of Cu leads for the case of finite Co slabs and those of Co leads in the case of semi-infinite Co leads.

The effect of quantum current oscillations was first studied by Mathon [14] using an empirical multiband TB-model within a Kubo-Landauer type approach by considering the dependence of the GMC on the thickness of the spacer. In Fig. 2 we present such calculations for $Co_5/Cu_s/Co_5$ trilayers with varying thickness of the spacer s. We clearly observe pronounced GMC oscillations (Fig. 2a) around a value of about 115% which are damped with increasing spacer thickness. It should be noted that in order to obtain converged results for the present case it is necessary to use a much finer sampling of the irreducible SBZ than mentioned above, namely 30000 $k_{||}$-points in the irreducible SBZ. A clearer picture is obtained by looking at the partial conductances, Fig. 2b. The

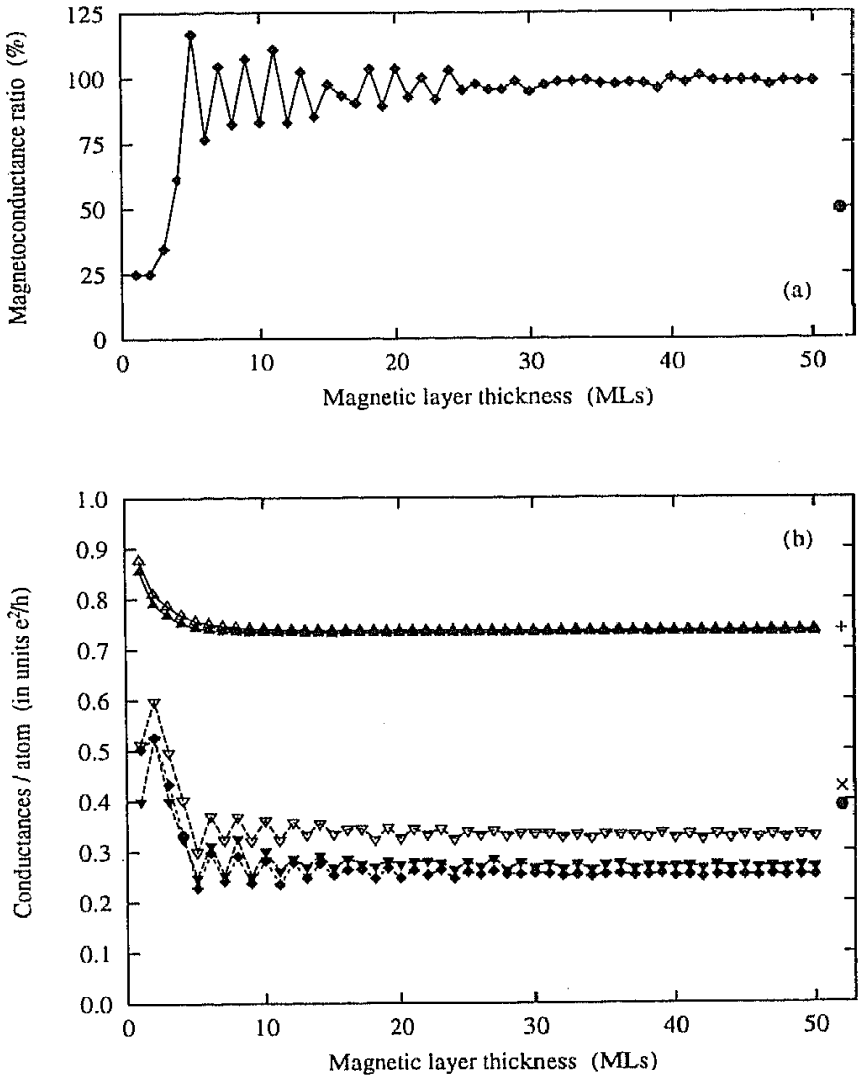

Figure 1 Ideal $Co_m/Cu_5/Co_m$ trilayers sandwiched by semi-infinite Cu leads as a function of the thickness of the magnetic slabs m: (a) magnetoconductance ratio (diamonds) and the limit of semi-infinite Co slabs (heavy dot); (b) conductances per atom for the ferromagnetic ↑-spin (up-triangles), ferromagnetic ↓-spin (down-triangles), and antiferromagnetic configuration (diamonds). Empty symbols (up- and down-triangles) refer to the ferromagnetic ↑- and ↓-spin conductances of a single Co slab of varying thickness embedded into a Cu host. For semi-infinite Co slabs the ferromagnetic ↑- (+), ↓- (×), and antiferromagnetic (heavy dot) conductances are shown, respectively.

oscillatory behavior originates mostly from the F↓-conductances whose amplitudes are much larger than those of the AF-conductances while the F↑-conductances are essentially thickness independent. We observe oscillations with a period of about 5–6 MLs in both the F↓- and AF-conductances while some admixture of short-period oscillations with a period of about 2.5 MLs is seen in the F↓-conductances. We note that these values correlate reasonably well with similar values obtained for the interlayer exchange coupling using the same electronic structure model

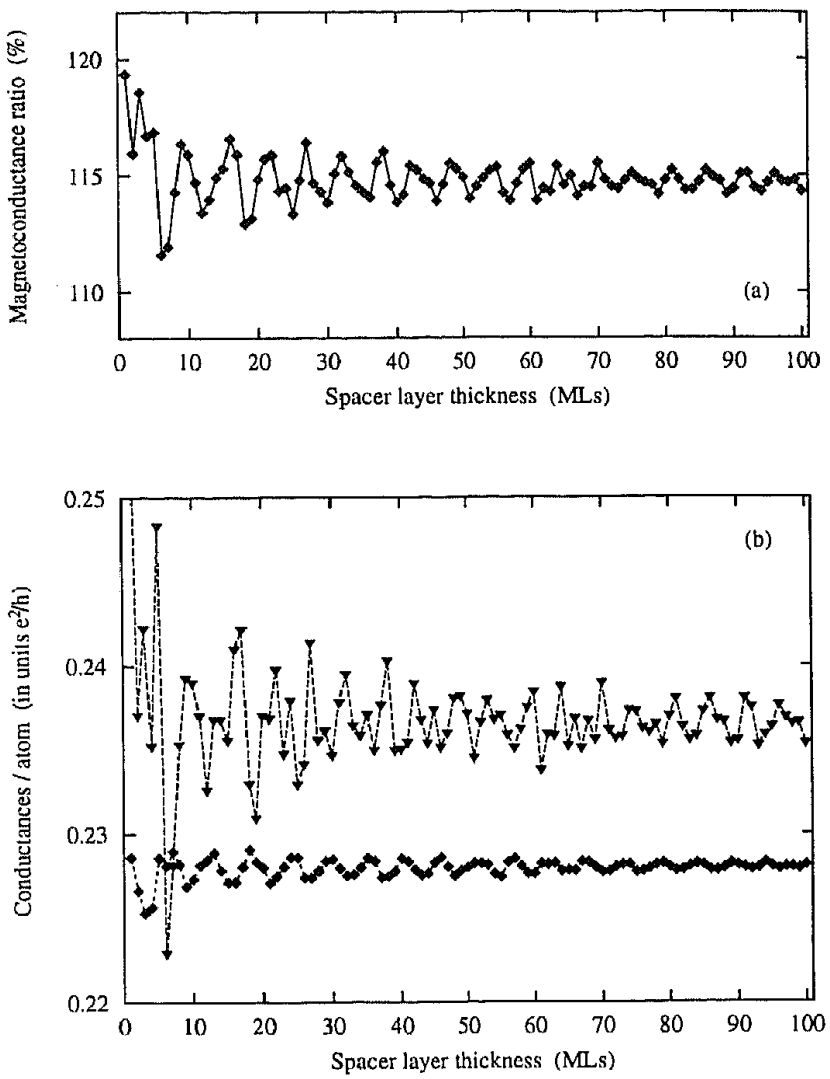

Figure 2 Ideal $Co_5/Cu_s/Co_5$ trilayers sandwiched by semi-infinite Cu leads as a function of the spacer thickness s: (a) magnetoconductance ratio (diamonds); (b) conductances per atom for the ferromagnetic $\downarrow$-spin (down-triangles) and antiferromagnetic configuration (diamonds). Note the reduced scale of y-axis.

(see, e.g., [21]). The amplitudes are roughly damped as s^{-1}, where s is the spacer thickness [14].

The oscillations of the GMC with respect to the spacer thickness s may also have an extrinsic origin rather than the intrinsic origin described above. In Fig. 3 we plot the dependence of the GMC as a function of the thickness of (CuPd) bilayers again sandwiched by Co slabs each 5 MLs thick. We have thus a superstructure in the spacer. The characteristic zig-zag shape of the GMC (Fig. 3a) is due to alternating Cu and Pd layers. By using this superstructure spacer we have combined magnetic (Co/Cu, for even numbers of spacer layers also Co/Pd) and non-magnetic (Cu/Pd) scattering at interfaces. The higher (smaller) values of the GMC correspond to the case of odd (even) numbers of spacer layers. The oscillations are clearly related to oscillations in the F$\uparrow$- and F$\downarrow$-conductances (Fig. 3b) which oscillate in phase giving rise

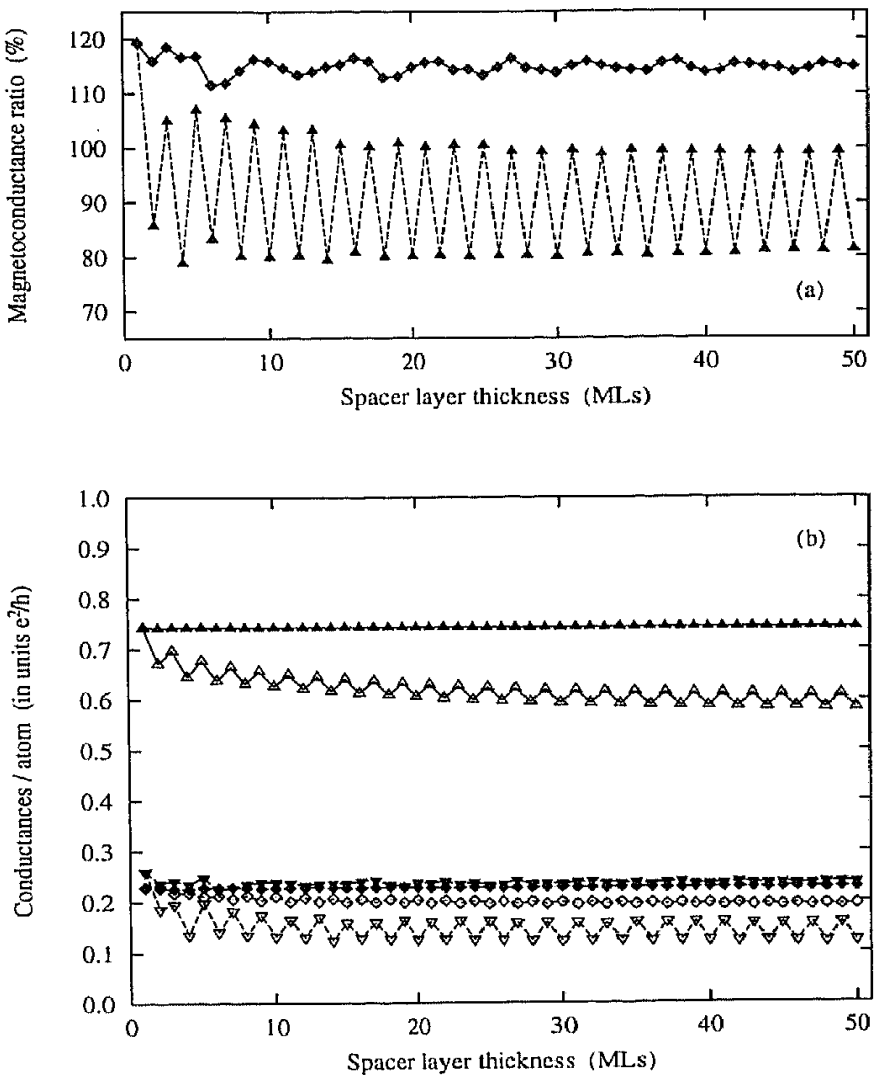

Figure 3 $Co_5/(CuPd)_r/Co_5$ and ideal $Co_5/Cu_s/Co_5$ trilayers sandwiched by semi-infinite Cu leads as a function of the spacer thicknesses s ($r = s/2$): (a) magneto-conductance ratio (diamonds, Cu spacer; triangles, (CuPd) spacer); (b) conductances per atom for the ferromagnetic ↑-spin (up-triangles), ferromagnetic ↓-spin (down-triangles), and antiferromagnetic configuration (diamonds). Full symbols refer to a Cu spacer, empty symbols to a (CuPd) spacer.

to an enhancement of oscillation amplitudes. It should be noted that as compared to the ideal trilayer the F↑- and F↓-conductances are reduced by the same amount. This fact indicates that the oscillations are now due to (dominating) non-magnetic scattering at the Cu/Pd interfaces rather than due to magnetic scattering at the Cu/Co interfaces as before (see Fig. 2b). The drop of the F- and AF-conductances can be understood in analogy to the interpretation given for Fig. 1b: the reason is a formation of an additional potential barrier in the d-channel due to a mismatch of Cu- and Pd-bands at the Fermi energy.

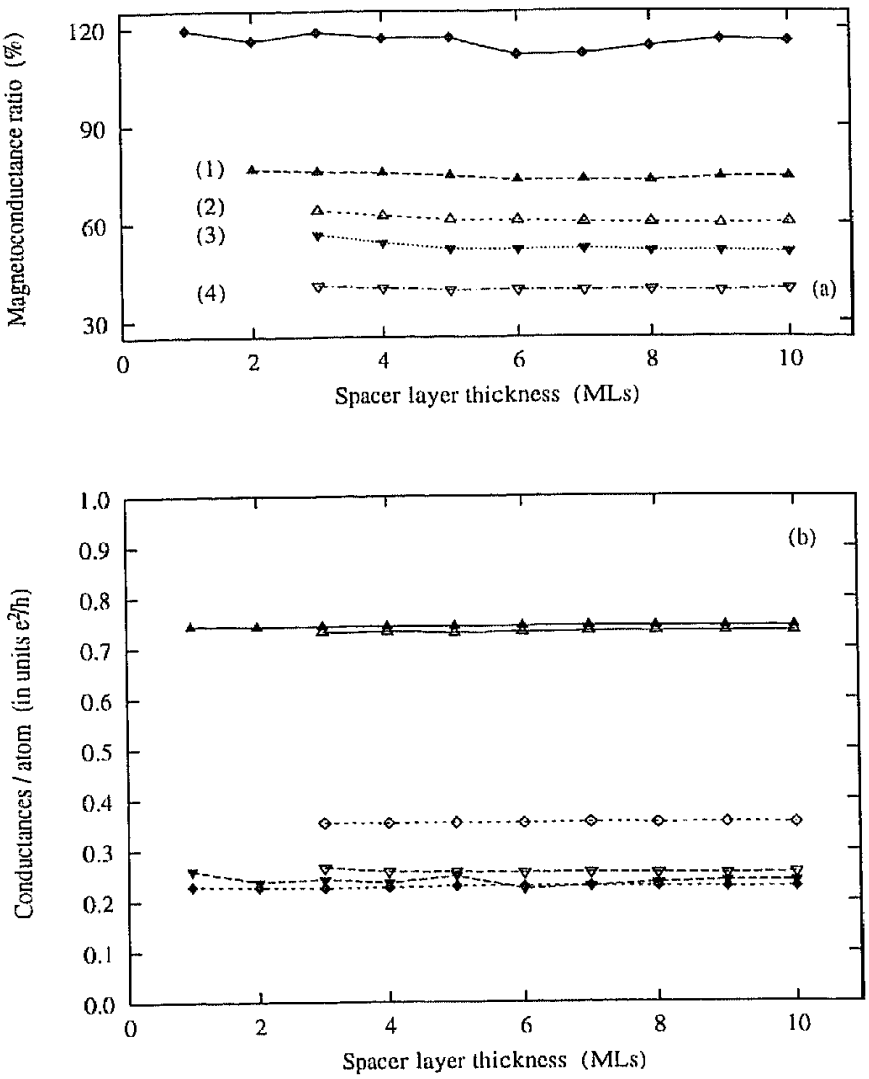

Figure 4 Trilayers with 15%-interdiffused interfaces and ideal $Co_5/Cu_s/Co_5$ trilayers sandwiched by semi-infinite Cu leads as a function of the spacer thickness s: (a) magnetoconductance ratio (diamonds, ideal trilayer; up-triangles-(1), one of the inner interfaces is interdiffused; empty up-triangles-(2), both inner interfaces are interdiffused; down-triangles-(3), two inner and one of outer interfaces are interdiffused; empty down-triangles-(4), all four interfaces are interdiffused); (b) conductances per atom for the ferromagnetic ↑-spin (up-triangles), ferromagnetic ↓-spin (down-triangles), and antiferromagnetic configuration (diamonds). Full symbols refer to an ideal trilayer, empty symbols to a trilayer with all interfaces interdiffused.

COMBINED BALLISTIC AND DIFFUSIVE TRANSPORT

In general, in addition to scattering at intrinsic defects (system interfaces) there is scattering at extrinsic defects, namely at impurities, stacking faults, dislocations, and there are even dynamical effects like scattering of electrons with phonons or magnons. Here we assume substitutional impurities in the spacer, magnetic slabs, and at their interfaces in a reference system which consists of the left and right semi-infinite Cu leads sandwiching two Co slabs, each 5 MLs thick, and separated by a Cu spacer of varying thickness (1-10 MLs).

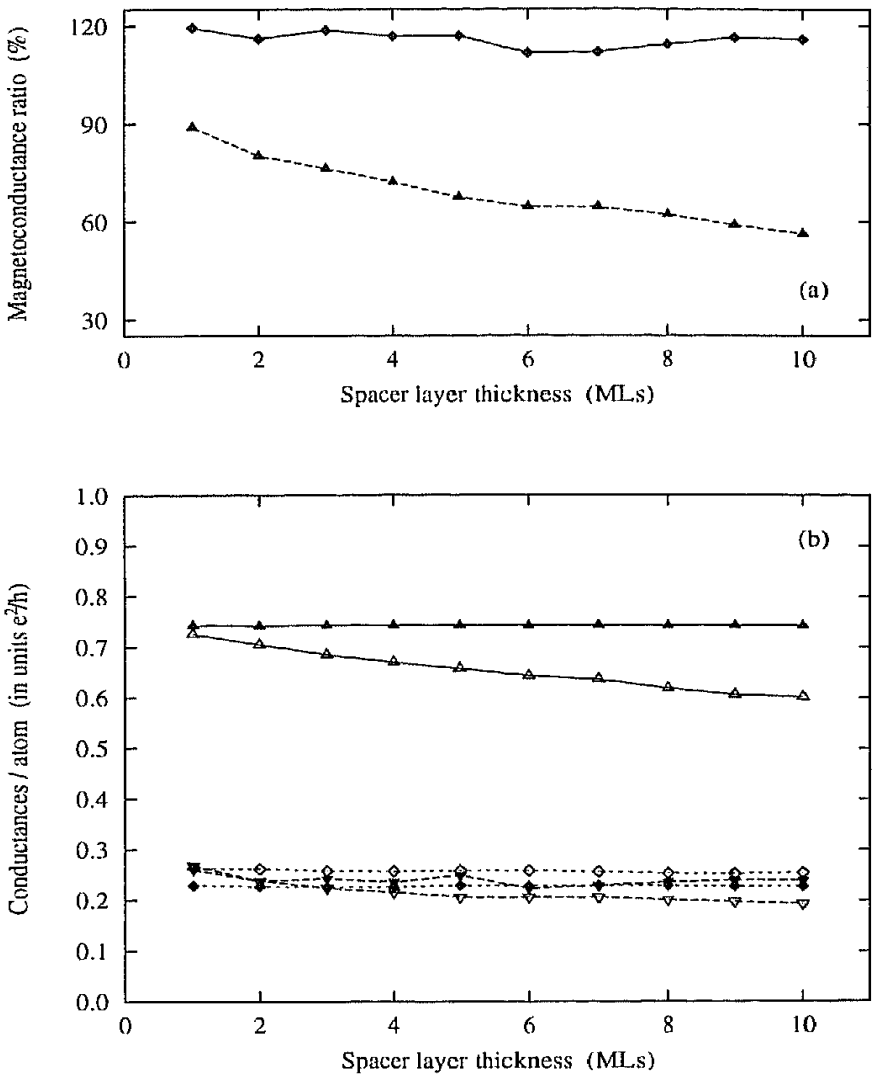

Figure 5 $Co_5/(Cu_{85}Ni_{15})_s/Co_5$ trilayers with alloyed spacer and ideal $Co_5/Cu_s/Co_5$ trilayers sandwiched by semi-infinite Cu leads as a function of the spacer thickness s: (a) magnetoconductance ratio (diamonds, ideal trilayer; triangles, alloyed spacer); (b) conductances per atom for the ferromagnetic ↑-spin (up-triangles), ferromagnetic ↓-spin (down-triangles), and antiferromagnetic configuration (diamonds). Full symbols refer to an ideal trilayer, empty symbols to a trilayer with alloyed spacer.

The effect of disorder at the Co/Cu interfaces is shown in Fig. 4. The interdiffused interface consists of two disordered interface layers with compositions $Co_{85}Cu_{15}$ (the Co side) and $Co_{15}Cu_{85}$ (the Cu side). The GMC decreases monotonically with the number of disordered interfaces, and disorder suppresses the oscillations present for an ideal interface. Disorder influences the F↑-conductances very weakly because of the similarity of the Cu- and the Co↑-bands. The AF-conductances, however, are much larger as compared to an ideal trilayer and their increase results in a decrease of the GMC. This behavior seems to contradict a common (but incorrect) belief that disorder always reduces the conductance. In fact, the effect of disorder is fourfold: (i) it increases the overall amount of scattering which contributes to the reduction of the transmis-

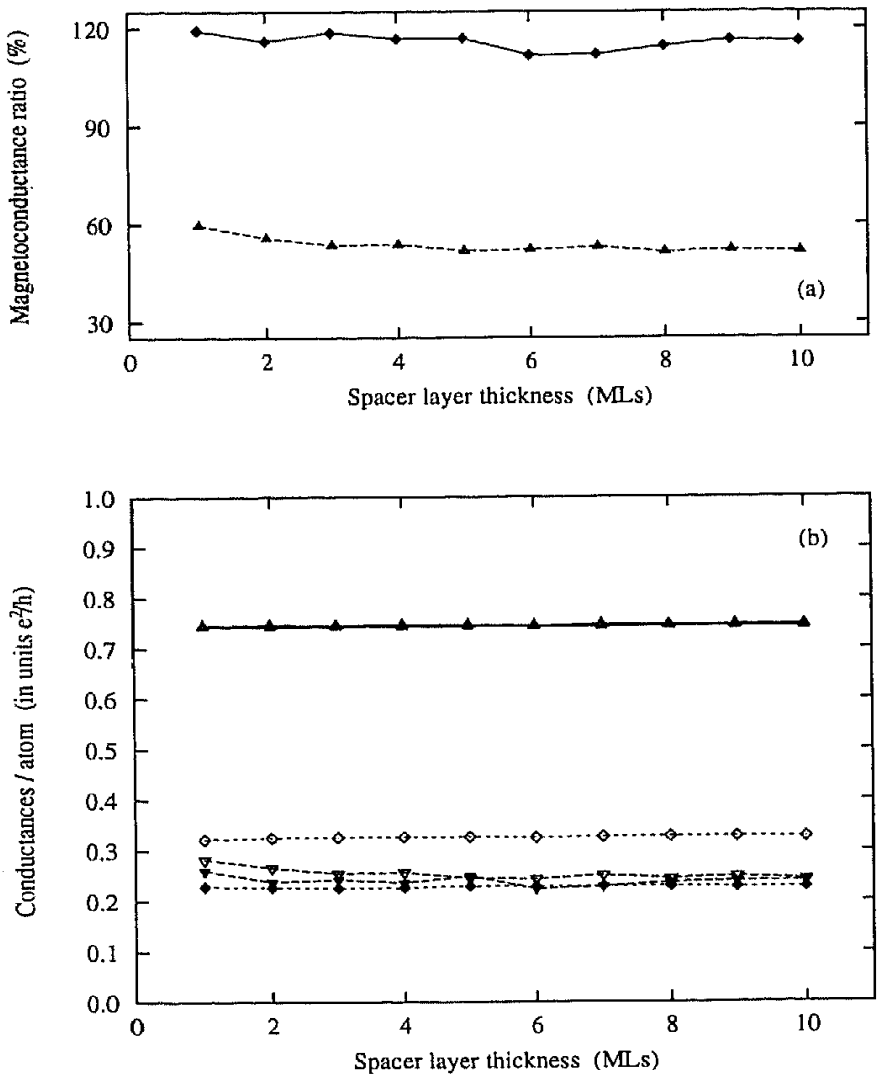

Figure 6 $(Co_{85}Ni_{15})_5/Cu_s/(Co_{85}Ni_{15})_5$ trilayers with alloyed magnetic slabs and ideal $Co_5/Cu_s/Co_5$ trilayers sandwiched by semi-infinite Cu leads as a function of the spacer thickness s: (a) magnetoconductance ratio (diamonds, ideal trilayer; triangles, alloyed magnetic slabs); (b) conductances per atom for the ferromagnetic $\uparrow$-spin (up-triangles), ferromagnetic $\downarrow$-spin (down-triangles), and antiferromagnetic configuration (diamonds). Full symbols refer to an ideal trilayer, empty symbols to a trilayer with alloyed magnetic layers.

sion probability and, hence, the conductance; (ii) the relaxation of a strict conservation of $\mathbf{k}_{||}$ in disordered systems opens up new transmission channels which contribute to an increase of the conductance; (iii) interdiffusion smoothes the abrupt potential barrier of the ideal trilayer which in turn also leads to an increased transmission coefficient; and (iv) the alloying in magnetic layers can increase (decrease) the effective barrier for $\uparrow$- and/or $\downarrow$-electrons at the Co/Cu interface and thus decrease (increase) the conductance in this channel. Therefore, the net influence of disorder on the conductance results from a competition between these effects and may lead to an increase or decrease of the conductance, depending on the system under consideration (see also [20]).

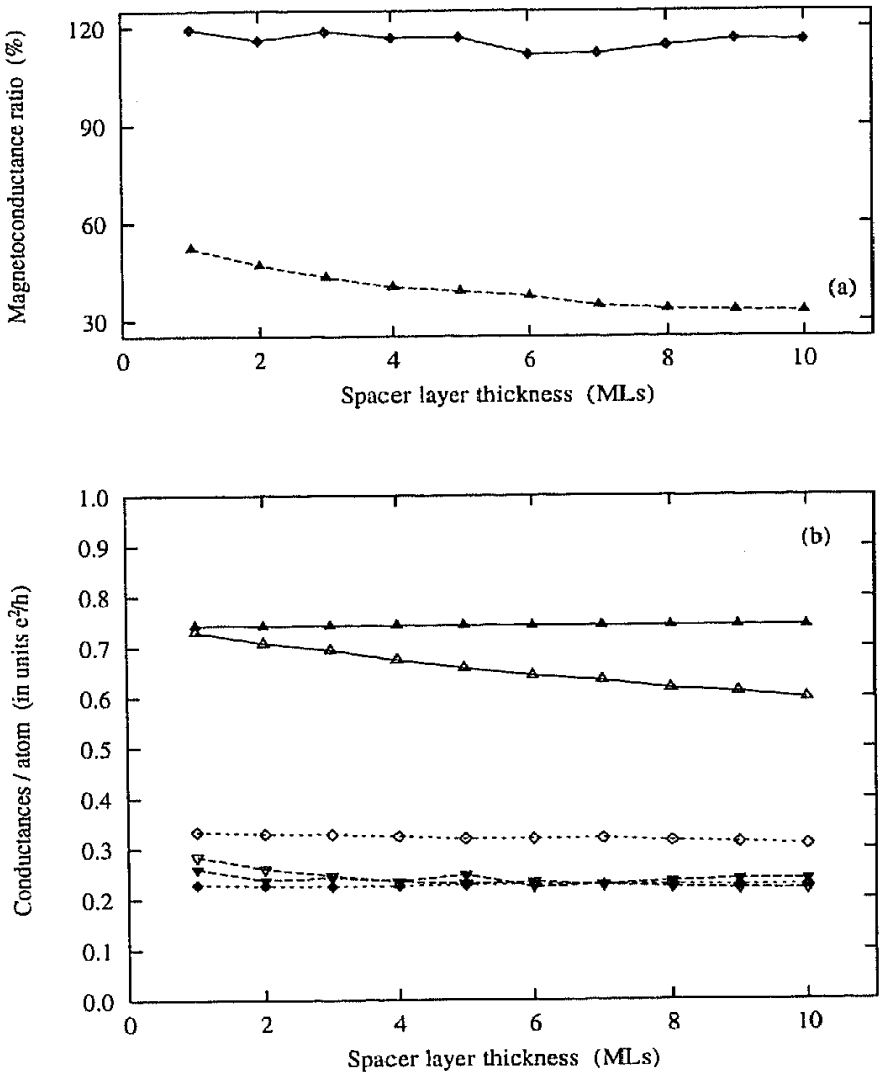

Figure 7 $(Co_{85}Ni_{15})_5/(Cu_{85}Ni_{15})_s/\ (Co_{85}Ni_{15})_5$ trilayers with combined alloying in both the spacer and magnetic slabs and ideal $Co_5/Cu_s/Co_5$ trilayers sandwiched by semi-infinite Cu leads as a function of the spacer thickness s: (a) magnetoconductance ratio (diamonds, ideal layer; triangles, alloyed magnetic slabs and spacer); (b) conductances per atom for the ferromagnetic ↑-spin (up-triangles), ferromagnetic ↓-spin (down-triangles), and antiferromagnetic configuration (diamonds). Full symbols refer to an ideal trilayer, empty symbols to an alloyed trilayer.

The effect of alloying in the non-magnetic spacer ($Cu_{85}Ni_{15}$) on the magnetoconductance is presented in Fig. 5. We observe a monotonic decrease of the GMC ratio as a function of the spacer thickness (Fig. 5a). The origin of this decrease can be traced from Fig. 5b. Disorder in CuNi alloys strongly depends on the concentration but for the Cu-rich alloys the states at the Fermi energy are influenced only weakly by disorder [22]. Therefore, the F↓- and AF-conductances are only slightly smaller than those of an ideal trilayer. Consequently, the effect of extrinsic potential scattering for the F↓- and AF-conductances is rather small as compared to the strong intrinsic scattering at the interfaces. On the other hand, the effect of extrinsic defects dominates the F↑-conductances where intrinsic scattering is negligibly small. In fact it is the F↑-channel

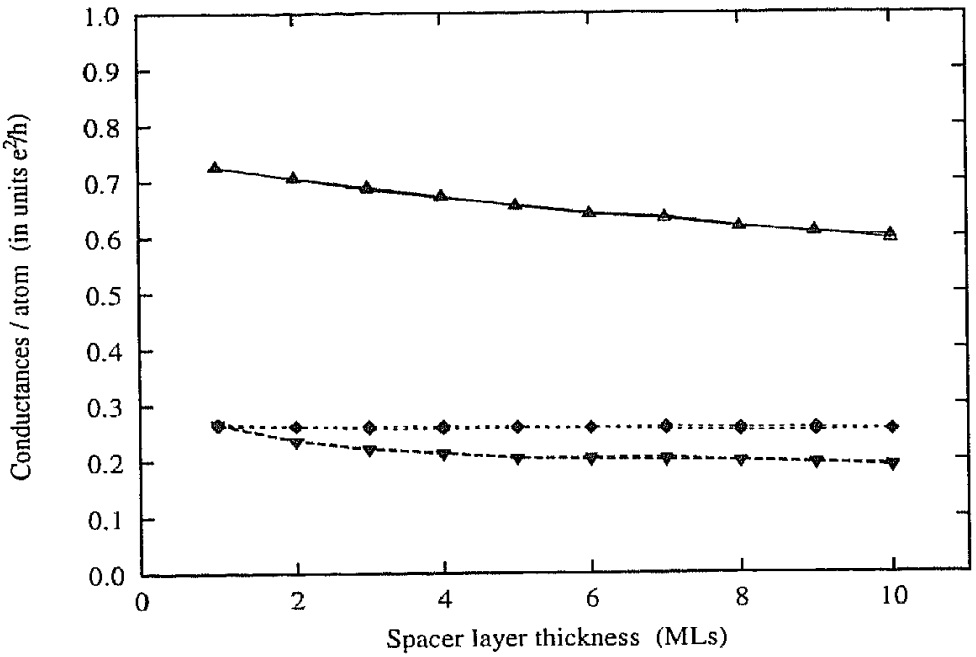

Figure 8 $Co_5/(Cu_{85}Ni_{15})_s/Co_5$ trilayers with alloyed spacer sandwiched by semi-infinite Cu leads as a function of the spacer thickness s: conductances per atom for the ferromagnetic ↑-spin (up-triangles), ferromagnetic ↓-spin (down-triangles), and antiferromagnetic configuration (diamonds). Full symbols refer to 5×5-supercell calculations, empty symbols to 7×7-supercell calculations.

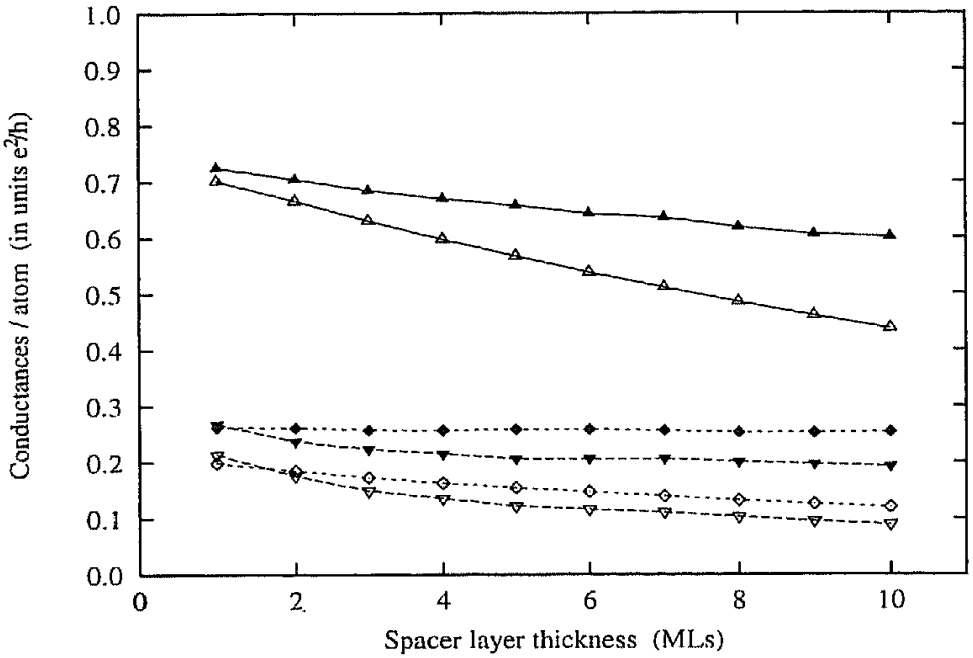

Figure 9 $Co_5/(Cu_{85}Ni_{15})_s/Co_5$ trilayers with alloyed spacer sandwiched by semi-infinite Cu leads as a function of the spacer thickness s: conductances per atom for the ferromagnetic ↑-spin (up-triangles), ferromagnetic ↓-spin (down-triangles), and antiferromagnetic configuration (diamonds). Full symbols refer to 5×5-supercell calculations, empty symbols to CPA calculations neglecting vertex corrections.

which is mostly responsible for the decrease of the GMC ratio with increasing spacer thickness.

The effect of alloying in the magnetic slabs ($Co_{85}Ni_{15}$) on the magnetoconductance is presented in Fig. 6. Contrary to the case of disorder in the spacer the GMC ratio quickly saturates to approximately half of the value for an ideal trilayer. The behavior of the partial conductances is similar to that for an interdiffused interface. The F↑-conductances are nearly the same as for the ideal trilayer due to the similarity of the Co↑- and the Ni↑-bands at the Fermi energy. Since the Co↓-bands are higher in energy as compared to the Ni↓-bands, alloying of Co with Ni decreases effectively the potential barrier height resulting thus into a larger transmission coefficient (conductance) as compared to the ideal trilayer. Consequently, the AF-conductances of the alloyed magnetic layers are larger than those of an ideal trilayer. The effect is the same for the F↓-conductances but much weaker, indicating dominating intrinsic scattering at interfaces for this channel.

The results of the study of combined disorder in both the spacer ($Cu_{85}Ni_{15}$) and the magnetic layers ($Co_{85}Ni_{15}$) are presented in Fig. 7. They are qualitatively similar to those for a random spacer but the GMC already starts at a value of about 60%, the value of disordered magnetic layers separated by an ideal Cu spacer (see Fig. 6). The decrease of the GMC is due to a corresponding decrease of the F↑-conductances resulting from alloying in the spacer.

Fig. 8 illustrates (for the case of partial conductances) the robustness of supercell calculations with respect to the supercell size and the configurational average (5×5-supercell averaged over five configurations versus 7×7-supercell averaged over three configurations). Illustrated here is the case of alloying in the spacer (in other cases the agreement is equally good). The good agreement between both calculations (number of atoms for the larger supercell increases two times) is obvious.

Finally, in Fig. 9, for the trilayer $Co_5/(Cu_{85}Ni_{15})_s/Co_5$ we compare the results of the supercell calculations with CPA-type transport calculations neglecting vertex corrections. In this limit we can still use the expression given by Eq. (8) but now specified to the 1×1-supercell case and with $g^{\beta,\sigma}_{1,N}(z)$ and $g^{\beta,\sigma}_{N,1}(z)$ substituted by $\left\langle g^{\beta,\sigma}_{1,N}(z)\right\rangle$ and $\left\langle g^{\beta,\sigma}_{N,1}(z)\right\rangle$, where $\langle\ldots\rangle$ denotes the CPA configurational averaging. The essence of the approximation thus consists in an independent configurational average of two Green functions keeping in mind that quantities $B^{\sigma}_{1}(E)$ and $B^{\sigma}_{N}(E)$ are related to non-random leads. The results now also depend on the choice of layers 1 and N between which we determine the conductance, i.e., the results neglecting vertex corrections which are based on Eqs. (8) and (13) are no longer identical. The CPA results are qualitatively similar to those obtained from the supercell calculations although

the CPA conductances are somewhat smaller, indicating perhaps that using a CPA-type approach vertex corrections ought to be included for CPP transport.

CONCLUSIONS AND OUTLOOK

We have presented an *ab initio* formulation of CPP transport in magnetic trilayers (spin valves). The approach is formulated within the framework of the TB-LMTO method and surface Green functions and can easily be generalized to lateral supercells, in particular since the lead supercell surface Green functions can be obtained from the surface Green function of the original two-dimensional lattice by means of a lattice Fourier transformation.

We have considered a number of interesting geometrical arrangements for both the ballistic and diffusive transport and discussed the results of the numerical calculations in terms of partial conductances of the ↑- and ↓-channels in the F and AF alignments. Although all calculations were done for the reference Co/Cu/Co(001) trilayer the present results have a broader validity because in quite a few binary magnetic systems the scattering in one spin channel can be significantly larger than in the other channel. We also discussed the effect of quantum oscillations of the magnetocurrent. Extensive numerical tests seem to indicate that already 5×5-supercells containing 25 atoms averaged over a limited number of random configurations (typically a configurational average over 5 different configurations was employed) give representative results for the CPP magnetoconductance. The present approach can also be generalized to the case of transport across a barrier (semiconductor or transition-metal oxide spacer or vacuum) as well as to the case of superconductor-metal interfaces.

Acknowledgments

Financial support for this work was provided by the Grant Agency of the Czech Republic (Project No. 202/97/0598), the Grant Agency of the Academy of Sciences of the Czech Republic (Project A1010829), the Center for Computational Materials Science in Vienna (GZ 45.442 and GZ 45.420), the Austrian Science Foundation (FWF P11626-PHY), the MŠMT of the Czech Republic (COST P3.70), the Austrian BMWV and the MŠMT of the Czech Republic (AKTION WTZ I.23), and the TMR Network 'Interface Magnetism' of the European Commission (Contract No. EMRX-CT96-0089).

REFERENCES

[1] M.N. Baibich, J.M. Broto, A. Fert, F. Nguyen Van Dau, F. Petroff, P. Etienne, G. Creuzet, A. Friedrich, and J. Chazelas, *Giant Magnetoresistance of (001)Fe/(001) Cr Magnetic Superlattices* Phys. Rev. Lett. **61**, 2472 (1988); G. Binasch, P. Grünberg, F. Saurenbach, and W. Zinn, *Enhanced Magnetoresistance in Layered Magnetic-Structures With Antiferromagnetic Interlayer Exchange* Phys. Rev. B **39**, 4828 (1989).

[2] W.P. Pratt Jr., S.-F. Lee, J.M. Slaughter, R. Loloee, P.A. Schroeder, and J. Bass, *Perpendicular Giant Magnetoresistances of Ag/Co Multilayers* Phys. Rev. Lett. **66**, 3060 (1991).

[3] P.M. Levy, Solid State Phys. **47**, 367 (1994).

[4] K.M. Schep, P.J. Kelly, and G.E.W. Bauer, *Ballistic transport and electronic structure* Phys. Rev. B **57**, 8907 (1998).

[5] M.A.M. Gijs and G.E.W. Bauer, *Perpendicular giant magnetoresistance of magnetic multilayers* Adv. Phys. **46**, 285 (1997).

[6] P. Zahn, I. Mertig, M. Richter, and H. Eschrig, *Ab-Initio Calculations of the Giant Magnetoresistance* Phys. Rev. Lett. **75**, 3216 (1995).

[7] D.R. Penn and M.D. Stiles, *Solution of the Boltzmann equation without the relaxation-time approximation* Phys. Rev. B **59**, 13338 (1999).

[8] W.H. Butler, X.-G. Zhang, D.M.C. Nicholson, and J.M. Mac Laren, *First-Principles Calculations of Electrical-Conductivity and Giant Magnetoresistance of Co-Vertical-Bar-Cu-Vertical-Bar-Co Spin Valves* Phys. Rev. B **52**, 13399 (1995).

[9] P. Weinberger, P.M. Levy, J. Banhart, L. Szunyogh, and B. Újfalussy, *'Band structure' and electrical conductivity of disordered layered systems* J. Phys.: Condens. Matter **8**, 7677 (1996); C. Blaas, P. Weinberger, L. Szunyogh, P.M. Levy, and C.B. Sommers, *Ab initio calculations of magnetotransport for magnetic multilayers* Phys. Rev. B **60**, 492 (1999).

[10] S. Datta, *Electronic Transport in Mesoscopic Systems* (Cambridge University Press, Cambridge, 1995).

[11] I. Turek, V. Drchal, J. Kudrnovský, M. Šob, and P. Weinberger, *Electronic Structure of Disordered Alloys, Surfaces and Interfaces* (Kluwer, Boston-London-Dordrecht, 1997).

[12] V. Drchal, J. Kudrnovský, and I. Turek, *Ab-initio calculations of the electronic and atomic structure of solids and their surfaces* Comput. Phys. Commun. **97**, 111 (1996).

[13] J.A. Stovneng and P. Lipavský, *Multiband Tight-Binding Approach to Tunneling in Semiconductor Heterostructures - Application to Gamma-X Transfer in GaAs* Phys. Rev. B **49**, 16494 (1994).

[14] J. Mathon, A. Umerski, and M. Villeret, *Oscillations with Co and Cu thickness of the current- perpendicular-to-plane giant magnetoresistance of a Co/Cu/Co(001) trilayer* Phys. Rev. B **55**, 14378 (1997).

[15] J. Cerdá, M.A. Van Hove, P. Sautet, and M. Salmeron, *Efficient method for the simulation of STM images. I. Generalized Green-function formalism* Phys. Rev. B **56**, 15885 (1997).

[16] S. Sanvito, C.J. Lambert, J.H. Jefferson, and A.M. Bratkovsky, *General Green's-function formalism for transport calculations with spd Hamiltonians and giant magnetoresistance in Co- and Ni-based magnetic multilayers* Phys. Rev. B **59**, 11936 (1999).

[17] P. Bruno, H. Itoh, J. Inoue, and S. Nonoyama, *Influence of disorder on the perpendicular magnetoresistance of magnetic multilayers* J. Mag. Mag. Mat. **198-199**, 46 (1999).

[18] E.Yu. Tsymbal and D.G. Pettifor, *Spin-polarized electron tunneling across a disordered insulator* Phys. Rev. B **58**, 432 (1998).

[19] F. James, *A Review of Pseudorandom Number Generators* Comput. Phys. Commun. **60**, 329 (1990).

[20] S. Zhang and P. Levy, *Interplay of the specular and diffuse scattering at interfaces of magnetic multilayers* Phys. Rev. B **57**, 5336 (1998).

[21] V. Drchal, J. Kudrnovský, I. Turek, and P. Weinberger, *Interlayer magnetic coupling: The torque method* Phys. Rev. B **53**, 15036 (1996).

[22] B.L. Gyorffy and G.M. Stocks, in *Electrons in Disordered Metals and at Metallic Surfaces*, eds. P. Phariseau, B.L. Gyorffy, and L. Scheire (NATO ASI Series, Plenum Press, New York, 1979).